Desalination and Water Treatment
www.deswater.com

doi: 10.1080/19443994.2015.1056833

57 (2016) 12335–12349
June

Taylor & Francis
Taylor & Francis Group

Basic Violet 10 (BV10) removal from aqueous solutions using sawdust of *Swietenia mahagoni* (Mahogany trees): adsorbent characterization, adsorption isotherm, kinetics, and thermodynamic studies

Nese Ertugay

Faculty of Engineering, Department of Civil Engineering, Erzincan University, 24100 Erzincan, Turkey, email: nertugay@erzincan.edu.tr

Received 14 July 2014; Accepted 27 April 2015

ABSTRACT

In this work, the adsorption potential of sawdust of *Swietenia mahagoni* to remove Basic Violet 10 (BV10) from aqueous solutions was investigated by batch adsorption system. The adsorbent was characterized by Fourier transform infrared spectrophotometer, scanning electron microscope, particle size distribution, and Brunauer, Emmett, and Teller methods. The effect of various experimental parameters such as pH, initial dye concentration, adsorbent concentration, and temperature on adsorption of BV10 was investigated. The optimum pH for BV10 adsorption was found to be 4.2. Equilibrium adsorption data were analyzed by the Langmuir, Freundlich, Temkin, and Scatchard isotherm models. The results show that the best fit was achieved with the Langmuir isotherm with a maximum adsorption capacity of 222.76 mg g^{-1} at 50°C. Pseudo-first-order, pseudo-second-order, intraparticle diffusion, and Elovich models were used to analyze the kinetic data obtained at different BV10 concentrations. The adsorption kinetic data were well described by the pseudo-second-order model. The calculated thermodynamic parameters, namely ΔG°, ΔH°, and ΔS°, showed that adsorption of BV10 was spontaneous and endothermic under examined conditions.

Keywords: Adsorption; Basic Violet 10; FTIR; BET; PSD; Kinetic

1. Introduction

Industrial wastewater usually contains a variety of organic compounds and toxic substances that are harmful to fish and other aquatic life [1]. During textile processing, large numbers of chemically different dyes appear in the form of wastewater and are directly discharged into the surrounding environment [2]. Dyes are usually of synthetic origin with complex aromatic molecular structures, which make them very stable, resistant to fading, and difficult to biodegrade [3]. As hazardous pollutants, they pose ecological risks and are toxic to aquatic life if discharged directly into receiving waters. They may be mutagenic and carcinogenic, and can cause a severe health hazard to human beings, such as dysfunction of kidneys, reproductive system, liver, brain, and central nervous system, and thus should be treated before discharging into the receiving body of water [4].

Today, there are more than 10,000 dyes with different chemical structures available commercially. Dyes are generally classified as anionic, cationic, and non-ionic depending on the ionic charge on the dye molecules. Among them, the cationic dyes are more toxic compared to anionic dyes, and their tinctorial values are very high (less than 1.0 mg L^{-1}) [5]. Basic dyes are a group of

water-soluble cationic dyes that are employed in leather, paper preparing, printing, and textile fibers dyeing [6].

Among a number of physicochemical dye treatment available, the adsorption technique has been proven to be one of the most promising for the removal of dyes from aqueous effluents. Activated carbon is one of the main adsorbents used to remove dyes from wastewater because of its good adsorption ability [7]. Activated carbon is the most widely used adsorbent for dye removal, but it is too expensive [8]. Various workers have been applied to remove basic dye such as palm kernel fiber [9], raw and pre-treated bentonite surfaces [10], succinylated sugarcane bagasse [11], *Hevea brasiliensis* seed coat [12], and bentonite [13].

The plant *Swietenia mahagoni* (L.) is a beautiful, lofty, evergreen large tree, 30–40 m high and 3–4 m in girth [14]. In the present study, the removal of Basic Violet 10 (BV10) was investigated in a batch system using sawdust of *S. mahagoni* as adsorbent. The effect of solution pH, adsorbent dosage, initial dye concentration, and temperature on BV10 removal was also studied. The adsorption isotherms, thermodynamics, and kinetics for both adsorbents were measured. Equilibrium data were fitted to Langmuir, Freundlich, Temkin, and Scathcard equations to determine the correlation between the isotherm models and experimental data.

2. Materials and methods

2.1. Adsorbate

BV10 dye, supplied from Fluka, was used without further purification. The chemical structure of BV10 is shown in Fig. 1. BV10 is CI = 45,170, chemical formula $C_{28}H_{31}ClN_2O_3$, FW = 479.02 gmol^{-1} [15], and λ_{max} = 553 nm. Stock dye solutions (1,000 mg L^{-1}) were prepared by dissolving 1 g of BV10 in 1 L of distilled water. Experimental solutions of desired concentration were obtained by further dilution. The spectrum of the BV10 at different dye concentrations shows an absorption peak at 553 nm as shown in Fig. 2.

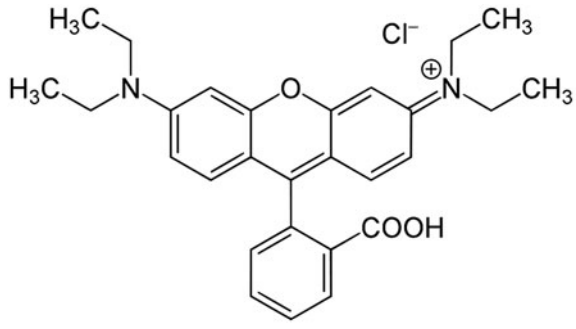

Fig. 1. Chemical structure of BV10 [16].

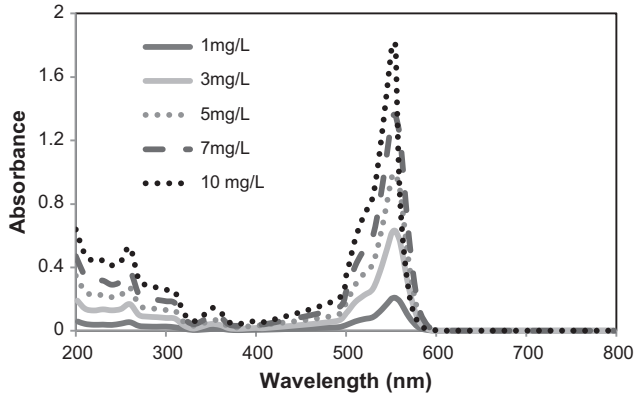

Fig. 2. UV–vis absorption spectrum of BV10.

2.2. Adsorbent and its characterization

Sawdust of *S. mahagoni* (mahogany trees) was obtained from a furniture factory. It was used directly for adsorption experiments without any treatment. Fourier transform infrared (FTIR) spectra were measured using Perkin–Elmer Spectrum One model FTIR spectrometer. The particle size distributions (PSD) of the solid samples were determined using a Malvern Mastersizer 2000 particle analyzer. The specific surface area and average pore size of the manure ash samples were analyzed by the Brunauer, Emmett, and Teller (BET) and BJH methods, respectively. The determinations of the surface area and pore size were based on isotherms of adsorption and desorption of nitrogen at 77 ± 0.5 K using a Gemini V2.00 Surface Analyzer (Micromeritics, USA). Before measurements, moisture and gases such as nitrogen and oxygen that were adsorbed on the solid surface or held in the open pores were removed under reduced pressure at 423 K for 7 h. Scanning electron microscopy was performed using a FEI model QUANTA FEG 450 instrument.

2.3. Batch adsorption studies

Adsorption studies were performed by the batch technique to obtain equilibrium data. Experiments were conducted in 250 mL erlenmeyer flasks containing known BV10 synthetic solutions. Flasks were agitated on a shaker at 240 rpm constant shaking rate for 160 min to ensure equilibrium was reached. The sample solutions were filtered at equilibrium using 0.45 μm filter paper to determine the residual concentrations. The residual concentration of the dye in the solution at different times of sampling was determined by UV–visible spectroscopy.

3. Results and discussion

3.1. Characteristics of the adsorbents

3.1.1. FTIR of sawdust of S. mahagoni

The BV10 adsorption onto sawdust of *S. mahagoni* is attributable to the functional groups and bonds present on them. In order to investigate the surface difference of adsorbent after and before adsorption, FTIR analyses were carried out in the range 400–4,000 cm^{-1}. Fig. 3 shows the infrared spectra of sawdust of *S. mahagoni* before and after BV10 adsorption. In FTIR spectra, the region between 3,200 cm^{-1} and 3,600 cm^{-1} showed a broad and strong band stretch, indicative of the presence of $-NH_2$ groups and free or hydrogen bonded O–H groups [17], indicating the presence of both surface-free hydroxyl groups and chemisorbed

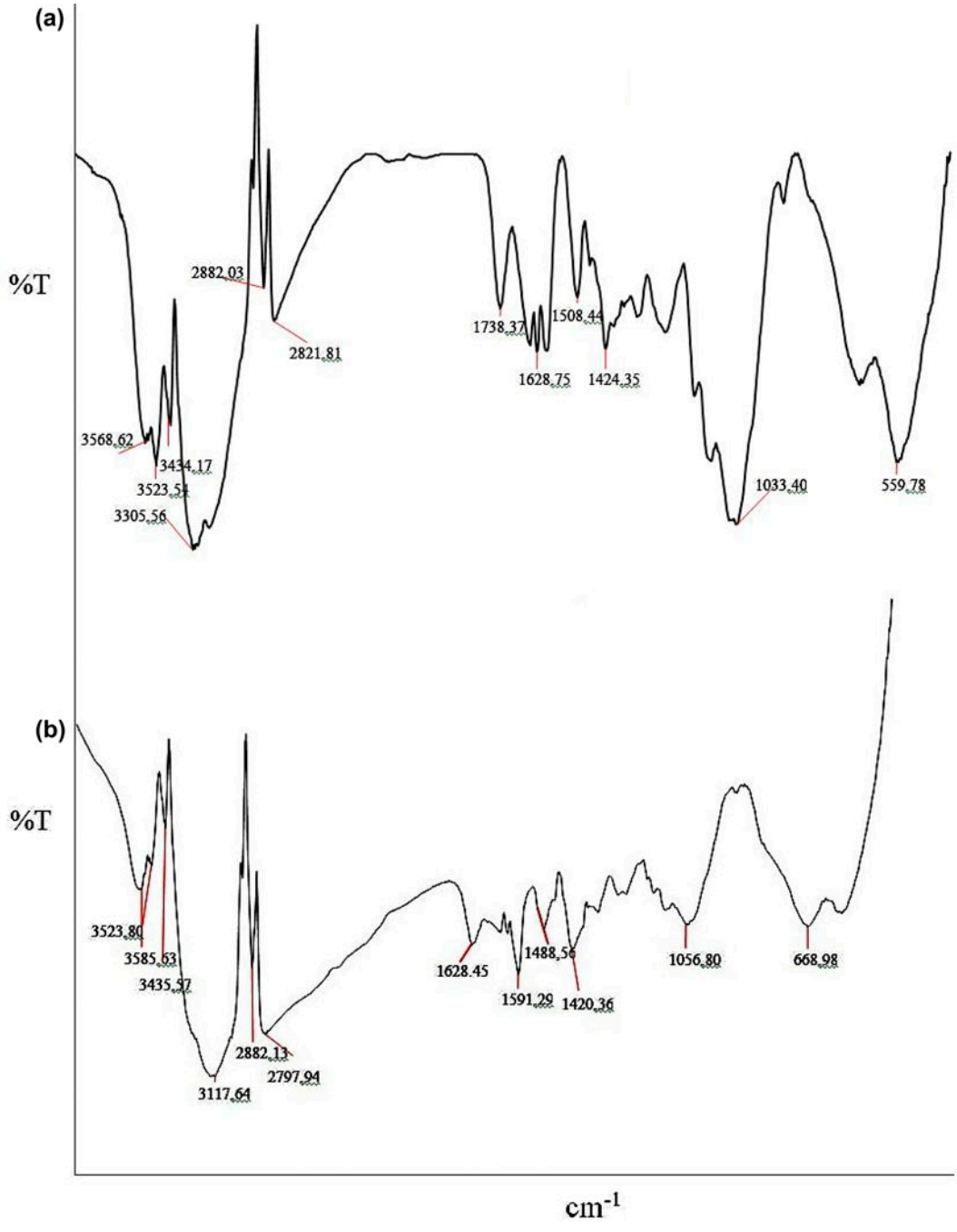

Fig. 3. FTIR spectra of sawdust of *S. mahagoni*: Initial sample before adsorption (a) and after adsorption (b) with BV10.

water on the adsorbent [18]. The absorption bands around 2,800 cm^{-1} were characteristic symmetric and asymmetric $–CH_2$ vibrations of sawdust of *S. mahagoni* [19]. The band observed at 1,738 cm^{-1} is relative to the carbonyl group (C=O) of carboxylic acid or ester [20]. The 1,738–1,508 cm^{-1} bands are associated with C=O stretching and C=C bonds, whereas the 1,424–1033 cm^{-1} band was assigned to the C–O and O–H bending modes [21] and the peaks shifted to 1,628–1,488 cm^{-1} and 1,420–1,056 cm^{-1} after the adsorption of BV10, respectively. The peak around 559 cm^{-1} corresponds to the –CN stretching [22]. There were clear band shifts and intensity decreases of the band at 1,738, 1,628, and 1,508 cm^{-1}. As shown in Fig. 3, the spectral analysis before and after BV10 adsorption indicated that O–H groups, $–NH_2$ groups, C–O and C=O stretching, C=C bonds, and –CN stretching were especially involved in dye adsorption.

3.1.2. Scanning electron microscope (SEM) of sawdust of S. mahagoni

Morphological differences between adsorbent before and after dye adsorption were examined by SEM techniques. In the present study, SEM photographs of sawdust of *S. mahagoni* reveal surface texture and porosity. The images showed clearly that, on the sample surfaces after adsorption, many grains of the dye ions accumulated on the surfaces of the samples but not deep within the pores as expected. Also, this figure reveals that the surface of sawdust of *S. mahagoni* is a rough surface. After dye adsorption, a significant change is observed in structure of the adsorbent Fig. 4(b) as a result of BV10 adsorption.

3.1.3. BET of sawdust of S. mahagoni

Fig. 5 displays nitrogen adsorption–desorption isotherms for pure sawdust of *S. mahagoni* and identified as the IV type isotherms according to Brunauer's classification [23]. Isotherms of sawdust are of IV type, which indicates the presence of mesopores. The hysteresis loop of the sample is of H4 type. Type H4

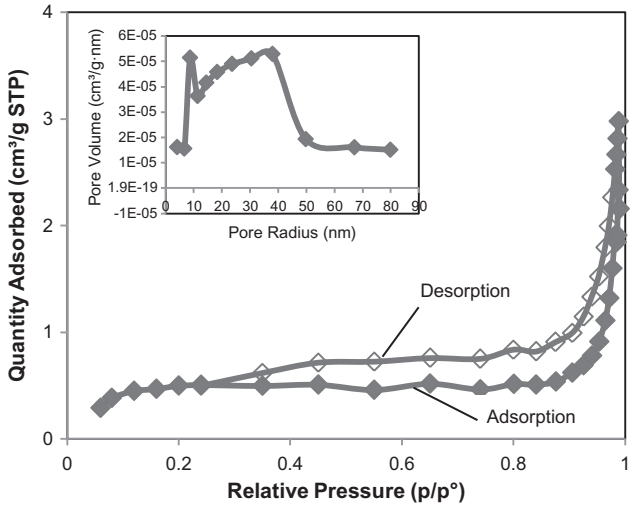

Fig. 5. N_2 adsorption–desorption isotherm and pore size distribution from BJH method of sawdust of *S. mahagoni*.

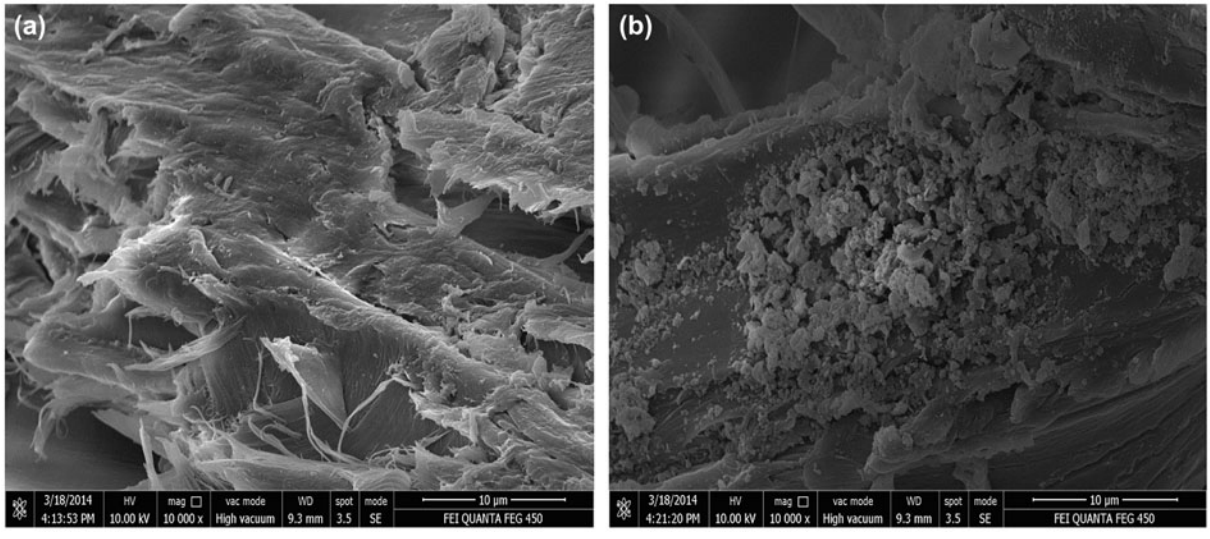

Fig. 4. SEM images of sawdust of *S. mahagoni* before (a) and after (b) dye adsorption.

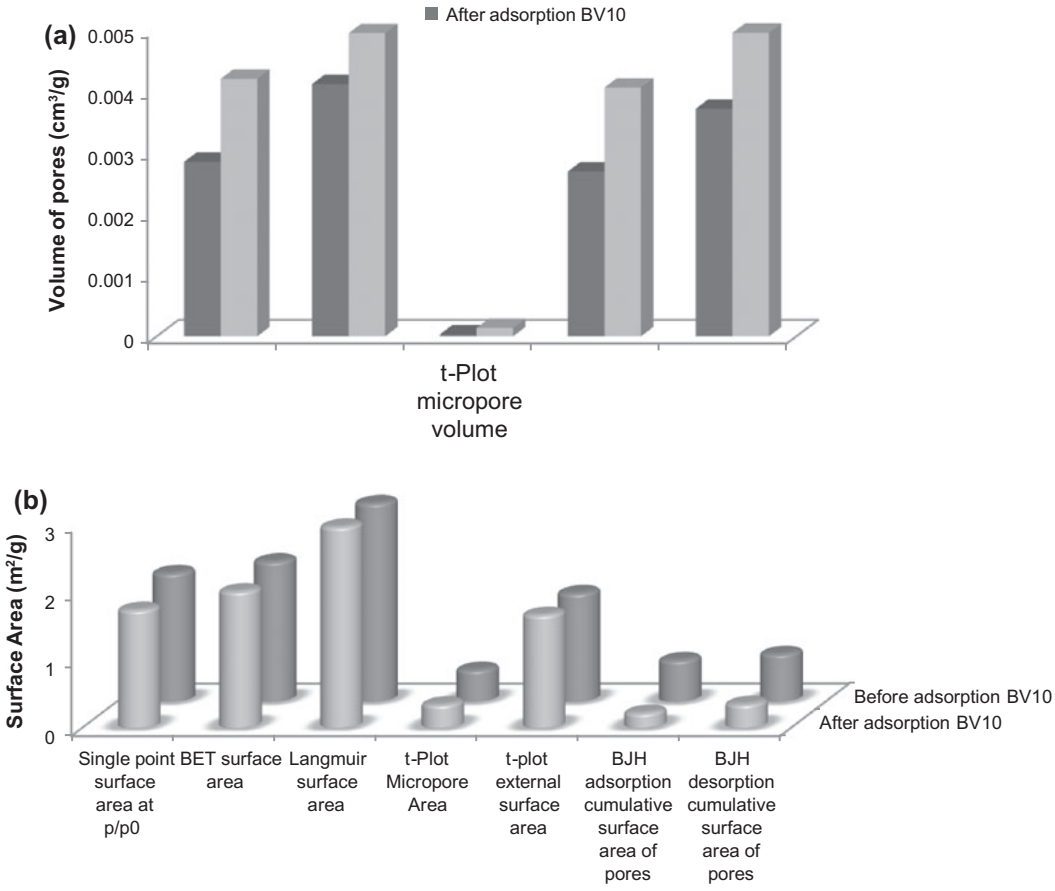

Fig. 6. (a) Pore volumes changes of sawdust and after BV10 adsorption and (b) surface areas changes of sawdust and after BV10 adsorption.

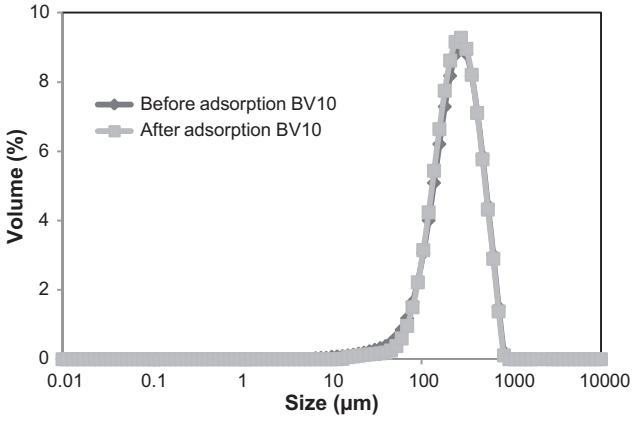

Fig. 7. Particle size distribution of sawdust of *S. mahagoni* before and after BY2 adsorption.

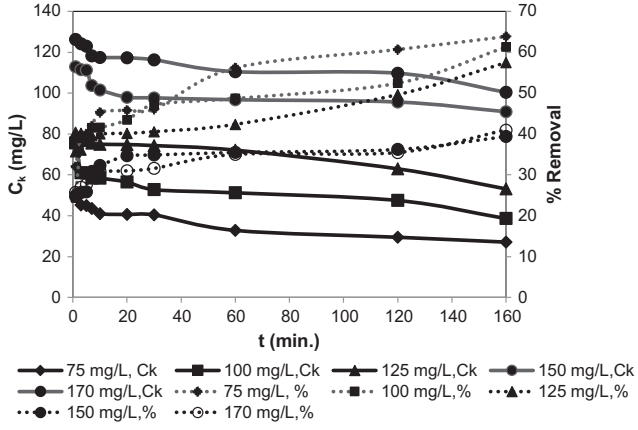

Fig. 8. Effect of the initial BV10 concentration on the adsorption by sawdust of *S. mahagoni*.

loops feature both parallel and almost horizontal branches. This occurrence has been attributed to adsorption–desorption in narrow slit-like pores [24]. Also, the pore size distribution from BJH method revealed mesoporosity (in Fig. 5). The classifications of pore sizes for micropores of less than 2 nm, mesopores (between 2 and 50 nm), and macropores (larger than 50 nm) were made [25]. The most probable pore size

was about 10–40 nm, according to Fig. 5, therefore it was regarded as a mesoporous material of sawdust of *S. mahagoni*.

According to Fig. 6(b), before BV10 adsorption, the specific BET and Langmuir surface area of sawdust of *S. mahagoni* was found to be 2.0686 m g^{-1} and 2.9282 m g^{-1} with corresponding total pore volume of 0.004957 cm g^{-1} ($P/P_0 = 0.98$). Micropore volume and micropore surface area were calculated using the t-plot method. The micropore surface area, calculated by the t-plot method, was 0.4682 m g^{-1} for sawdust.

Also, for sawdust of *S. mahagoni*, BJH adsorption/desorption surface area of pores is 0.611/0.7037 $m^2 g^{-1}$ and cumulative adsorption/desorption pore volume of the pores is 0.004068/0.004962 $cm^3 g^{-1}$, respectively.

As seen in Fig. 6(a) and (b), values of pore volume and surface area after BV10 dye adsorption were decreased. This situation is due to the attachment of dye molecules into pores and BV10 adsorption occurring.

3.1.4. PSD of sawdust of S. mahagoni

Particle size distribution of sawdust of *S. mahagoni* shows a satisfactory bell-shaped distribution curve (Fig. 7). The particle size distribution analysis shows that the sizes of sawdust particles are in the range of 10–800 μm. Before BV10 adsorption, the sample contains 10% particles of diameters smaller than 109.129 μm, 50% particles of diameters smaller than 267.824 μm and 90% particles of diameters smaller than 537.398 μm. The mean diameter of its particles in the whole sample volume (D[3,4]) is 298.354 μm. After BV10 adsorption, the sample contains 10% particles of diameters smaller than 119.782 μm, 50% particles of diameters smaller than 267.534 μm and 90% particles of diameters smaller than 531.238 μm. The mean diameter of its particles in the whole sample volume (D[3,4]) is 299.353 μm.

3.2. Effect of initial BV10 concentration on adsorption by sawdust of S. mahagoni

The initial dye concentration provides an important driving force to overcome all mass-transfer resistances of dyes between the aqueous and solid phases [7]. The adsorption of BV10 onto sawdust of *S. mahagoni* at various initial dye concentrations (75–170 mg L^{-1}) was studied as a function of contact time in order to determine the necessary adsorption equilibrium time. Fig. 8 shows the effect of contact time and initial BV10 concentration on adsorption sawdust of *S. mahagoni*. As shown in Fig. 8, adsorption at different initial BV10 concentrations is rapid at the initial stages and then gradually decreases with the progress of adsorption until the equilibrium is reached. For the adsorption experiments, an equilibrium time of 160 min was considered to be optimum. The rapid adsorption at the initial contact time is due to the availability of the negatively charged surface of adsorbent which led to fast electrostatic adsorption of the cationic dye molecules from the solution. Afterwards with the gradual occupancy of these sites, the adsorption became less efficient and dye needed to diffuse to the sorbent surface [26].

It was observed that the removal of BV10 increased with decreases in initial dye concentration. The residual dye concentration (C_k) increased from 27 to 100 mg L^{-1} when the initial BV10 concentration increased from 75 to 170 mg L^{-1} at room temperature. Contrarily, the dye removal decreased from 63.86 to 40.93% when the initial BV10 concentration increased from 75 to 170 mg L^{-1} at room temperature.

3.3. Effect of solution pH on adsorption by sawdust of S. mahagoni

The pH of the dye solution is an important factor for the sorption capacity of sorbate molecule due to its influence on both characteristics of sorbent surface and ionization of the dyestuff molecule [27]. The effect of solution pH on the BV10 removal was studied at different initial pH values (2.5–6.0) and is shown in Fig. 9 as decrease in absorbance. As shown in Fig. 9, the most decrease in absorbance of 100 mg L^{-1} BV10 concentrations was obtained at natural pH. Also, the percentages of dye removal by sawdust of *S. mahagoni* were found to be 54, 50.8, 59.2, 45.7, and 54.2% at pH of 2.5, 3.5, 4.2,

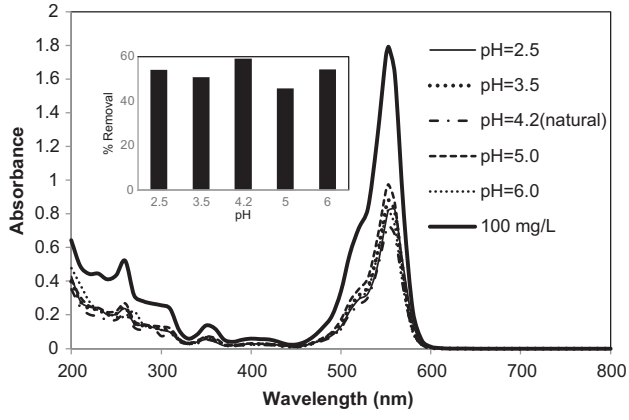

Fig. 9. Effect of solution pH on the adsorption by sawdust of *S. mahagoni*.

5.0, and 6.0, respectively. According to the results, pH 4.2 (natural pH of adsorbent) was chosen as the optimum pH for removal of BV10 for further experiments.

3.4. Effect of adsorbent concentration on adsorption by sawdust of S. mahagoni

One of the parameters that strongly affects sorption capacity is the quantity of contacting sorbent in the liquid phase [28]. Fig. 10 shows the effect of adsorbent dose on the percentage removal of BV10 by sawdust of *S. mahagoni* as adsorbent. This figure reveals that the removal of BV10 increased up to a certain adsorbent dosage and then decreased. An increase in adsorption with adsorbent dosage can be attributed to increased surface area and the availability of more adsorption sites [29]. The percentage of BV10 removal increased from 33.4 to 59.2% as the adsorbent dose increased from 0.5 to 1.0 g L^{-1} and then when adsorbent dosage was 1.5 mg L^{-1}, percentage of BV10 removal decreased to a value of 41%. The reason for this is the increase of adsorbent dosage may be attributed to saturation of adsorption sites due to particulate interaction such as aggregation. Such aggregation would lead to a decrease in total surface area of the adsorbent and increase in diffusional path length [30]. Also, adsorption capacity of BV10 increased from 39.33 to 133.2 mg g^{-1} with the decreasing sawdust of *S. mahagon*i concentration from 1.5 to 0.5 g L^{-1}. Therefore, the adsorbent dose was fixed at 0.5 g L^{-1} at all experiments.

3.5. Effect of temperature on adsorption by sawdust of S. mahagoni

The effects of temperature on adsorption and removal of BV10 were studied at 20, 30, 40, and 50°C and sawdust of *S. mahagoni* showed maximum dye adsorption at 50°C and the least adsorption at 20°C. An increase in the BV10 adsorption capacity and removal occurred when the temperature increased (Fig. 11). This may be due to the higher rate of diffusion of BV10 onto the adsorbent surface particle at higher temperatures [3]. It can be seen that there is a marked increase from 110 to 169.66 mg g^{-1} in the adsorption capacity of BV10 as temperature increases, indicating the endothermic nature of the adsorption reaction of BV10 onto sawdust of *S. mahagoni* [4].

3.6. Adsorption equilibrium studies

Equilibrium data, commonly known as adsorption isotherms, describe how the adsorbate interacts with adsorbents, and give a comprehensive understanding of the nature of interaction. It is basically important to optimize the design of an adsorption system [4]. The parameters and correlation coefficients obtained from the plots of Freundlich ($\ln q_e$ vs. $\ln C_e$), Langmuir (C_e/q_e vs. C_e), Temkin (q_e vs. $\ln C_e$), and Scatchard isotherms (q_e/C_e vs. q_e) at different temperatures are listed in Table 1.

As shown in Table 1, the Langmuir isotherm model fitted better with higher R^2 values compared to the other isotherm models. Conformation of the experimental data into Langmuir isotherm equation indicated the homogeneous nature of sawdust of *S. mahagoni* surface, i.e. each dye molecule/sawdust adsorption had equal adsorption activation energy. Additionally, the results demonstrated the formation of monolayer coverage of dye molecule at the outer surface of sawdust of *S. mahagoni* [31].

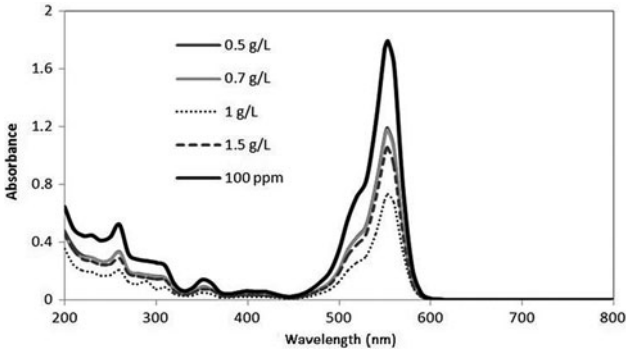

Fig. 10. Effect of adsorbent dosage on the adsorption by sawdust of *S. mahagoni*.

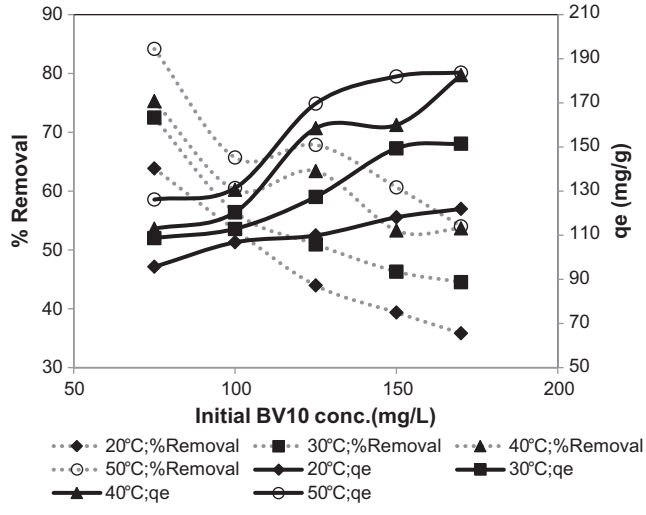

Fig. 11. Effect of temperature on the adsorption by sawdust of *S. mahagoni*.

Table 1
Isotherm constants for BV10 adsorption on sawdust of *S. mahagoni* at different temperatures

Type		20℃	30℃	40℃	50℃
$\frac{C_e}{q_e}=\frac{1}{Q_0K}+\frac{C_e}{Q_0}$	Langmuir isotherm				
Q_0 (mg g^{-1})		6.43	178.57	212.22	222.76
K (Lg^{-1})		1.135	0.052	0.043	0.083
R^2		0.9923	0.9657	0.9161	0.9604
$\ln q_e=\ln K_f+\frac{1}{n}C_e$	Freundlich isotherm				
K_F (Lg^{-1})		90.90	94.81	98.03	117.97
n		357.14	196.08	129.87	158.73
R^2		0.9505	0.9397	0.8251	0.7714
$q_e=B\ln A+B\ln C_e$	Temkin isotherm				
B		18.12	29.87	33.28	37.93
A (Lg^{-1})		7.28	1.47	1.03	3.07
R^2		0.9719	0.8177	0.6984	0.7520
$\frac{q_e}{C_e}=K_sQ_s-K_sq_e$	Scatchard isotherm				
K_s (L mg^{-1})		0.0925	0.0573	0.0392	0.0877
Q_s (mg g^{-1})		131.81	176.77	234.81	213.55
R^2		0.9261	0.5843	0.5337	0.5366

In the Freundlich adsorption isotherm, the value of K_F increased with temperature, indicating that adsorption capacity increases with temperature. As can be further seen from Table 1, the values of Q_o and K_F increased with temperature, indicating that the adsorption process was endothermic in nature. The maximum adsorption capacity based on the Langmuir isotherm was 222.76 mg g^{-1} at 50℃. The maximum adsorption capacity was found to increase from 6.43 to 222.76 mg g^{-1} for an increase in the solution temperatures from 25 to 45℃.

The essential characteristics of the Langmuir isotherm may be expressed in terms of dimensionless separation parameters R_L, which is indicative of the isotherm shape that predicts whether an adsorption system is favorable or unfavorable. R_L is defined as (Eq. (1)):

$$R_L=\frac{1}{1+KC_0} \quad (1)$$

where K_L and C_o are the Langmuir constant and initial BV10 concentration, respectively [1]. The R_L value indicates the type of the isotherm to be either favorable ($0 < R_L < 1$), unfavorable ($R_L > 1$), linear ($R_L = 1$), or irreversible ($R_L = 0$) [15]. As shown in Fig. 12, R_L values were in the range of 0.0052–0.2367 indicating that the adsorption was favorable.

The Temkin isotherm constant in Table 1 shows that the heat of adsorption (B) increases with increasing temperature, indicating endothermic adsorption. The shape of the Scatchard plot is related to the type of the interactions of adsorbate with adsorbent.

3.7. Adsorption kinetics

In order to analyze the adsorption kinetics of BV10, the pseudo-first-order, pseudo-second-order, intraparticle diffusion, and Elovich models were applied to experimental data. The values of constants obtained from kinetics are given in Table 2.

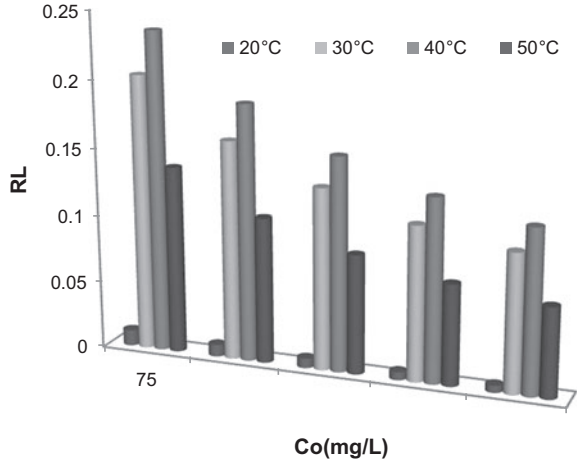

Fig. 12. R_L values at different temperatures relating to the initial BV10 concentrations.

Table 2
Kinetic parameters for the adsorption of BV10 onto sawdust of *S. mahagoni* at different initial BV10 concentrations and temperatures

BV10 conc. (mgL^{-1})	$q_{e,exp}$ ($mg\,g^{-1}$)	Pseudo-first-order kinetic			Pseudo-second-order kinetic				Intraparticle diffusion			Elovich Equation		
		$q_{e,cal}$ ($mg\,g^{-1}$)	k_1 ($L\,min^{-1}$)	R^2	$q_{e,cal}$ ($mg\,g^{-1}$)	$k_2\ 10^{-3}$ (mg/(g min))	R^2	$h = k_2 q_e^2$ (mg/(g min))	k_i ($mg/g\,min^{1/2}$)	C	R^2	a	b	R^2
20°C														
75	95.8	39.4	0.018	0.9697	96.1	1.05	0.9957	19.32	3.66	51.66	0.9461	3.10^3	0.112	0.9437
100	106.9	33.8	0.024	0.9350	107.5	3.26	0.9990	37.73	3.57	67.57	0.7284	7.10^3	0.102	0.9121
125	110	15	0.017	0.8858	109.9	7.59	0.9997	91.65	1.56	91.85	0.8354	2.10^5	0.250	0.9470
150	118.2	29.8	0.012	0.6243	116.3	3.52	0.9973	47.62	3.32	78.72	0.7624	2.10^4	0.110	0.9007
170	122	27.6	0.027	0.9271	123.5	4.32	0.9996	65.79	2.82	90.94	0.8600	2.10^6	0.130	0.9513
30°C														
75	108.8	30.8	0.024	0.9650	109.9	3.55	0.9992	42.92	3.04	74.53	0.9004	4.10^4	0.129	0.9768
100	112.9	24	0.012	0.7511	111.1	4.43	0.9983	54.64	2.54	82.35	0.8078	4.10^5	0.148	0.9586
125	127.4	19.8	0.029	0.9582	128.2	6.68	0.9998	109.89	1.84	106.86	0.9015	5.10^8	0.214	0.9762
150	149.4	25.8	0.014	0.6585	136.9	4.63	0.9991	86.96	3.05	104.24	0.7344	2.10^6	0.121	0.9070
170	151.5	34.2	0.019	0.9373	151.5	3.23	0.9993	74.07	3.52	111.14	0.8806	9.10^5	0.109	0.995
40°C														
75	113	21.8	0.017	0.9659	112.4	4.80	0.9992	60.61	2.07	88.08	0.9444	8.10^7	0.195	0.9702
100	120.5	20.4	0.008	0.6026	117.7	4.85	0.9974	67.12	1.97	94.39	0.7319	4.10^7	0.189	0.8789
125	158.6	19.1	0.009	0.4947	156.3	5.94	0.9988	144.92	2.01	133.13	0.7366	8.10^9	0.181	0.9096
150	160	45.7	0.023	0.8858	161.3	2.43	0.9993	63.29	4.95	105.40	0.8421	2.10^4	0.080	0.9789
170	182.6	50	0.006	0.8383	175.4	1.50	0.9891	46.30	3.86	123.56	0.8631	5.10^6	0.111	0.7710
50°C														
75	126.2	23.2	0.012	0.6982	125.0	5.14	0.9985	70.92	2.44	96.49	0.7953	9.10^6	0.154	0.9270
100	131.4	10.7	0.016	0.5185	131.6	1.30	0.9999	227.28	1.68	113.89	0.4862	6.10^8	0.192	0.7709
125	169.7	38.8	0.013	0.8000	166.7	2.63	0.9984	72.99	4.05	121.08	0.7795	4.10^5	0.090	0.9164
150	181.9	36.7	0.012	0.9433	178.6	2.64	0.9983	84.03	3.63	138.71	0.9687	2.10^8	0.125	0.9534
170	183.7	42.5	0.020	0.9778	185.2	2.49	0.9993	85.46	4.11	138.78	0.9451	4.10^6	0.098	0.9779

Linear form of pseudo-first-order kinetic equation is expressed as (Eq. (2)):

$$\log (q_e - q_t) = \log q_e - \frac{k_1}{2.303} t \quad (2)$$

where q_e (mg g^{-1}) is the amount of dye adsorbed at the point of equilibrium, q_t (mg g^{-1}) is the amount of dye adsorbed at time t, and k_1 (1 min^{-1}) is the rate constant which can be calculated from the straight line plot of log ($q_e - q_t$) vs. time [2] (in Fig. 13).

Linear form of pseudo-second-order kinetic equation is expressed as (Eq. (3)):

$$\frac{t}{q_t} = \frac{1}{k_2 q_e^2} + \frac{1}{q_e} t \quad (3)$$

Equilibrium adsorption capacity q_e and second-order constants k_2 can be determined experimentally from the slope and intercept of plot t/q_t vs. t [32] (in Fig. 14).

Since the above kinetic models cannot describe the intraparticle diffusion, the intraparticle mass-transfer diffusion model was studied. It is described using the following (Eq. (4)):

$$q_t = k_i t^{1/2} + C \quad (4)$$

where k_i (mg/g min$^{1/2}$) is the intraparticle diffusion rate constant and C (mg g^{-1}) is the intercept [33] (in Fig. 15). When $C = 0$, the adsorption kinetics are controlled only by intraparticle diffusion. If $C \neq 0$, the adsorption process is quite complex [34].

The Elovich equation generally used is expressed as [35]:

$$q_t = \frac{1}{b} \ln(ab) + \frac{1}{b} \ln t \quad (5)$$

where q_t (mg g^{-1}) is the amount of dye adsorbed at time t (min) and a and b are the constants. The chemical

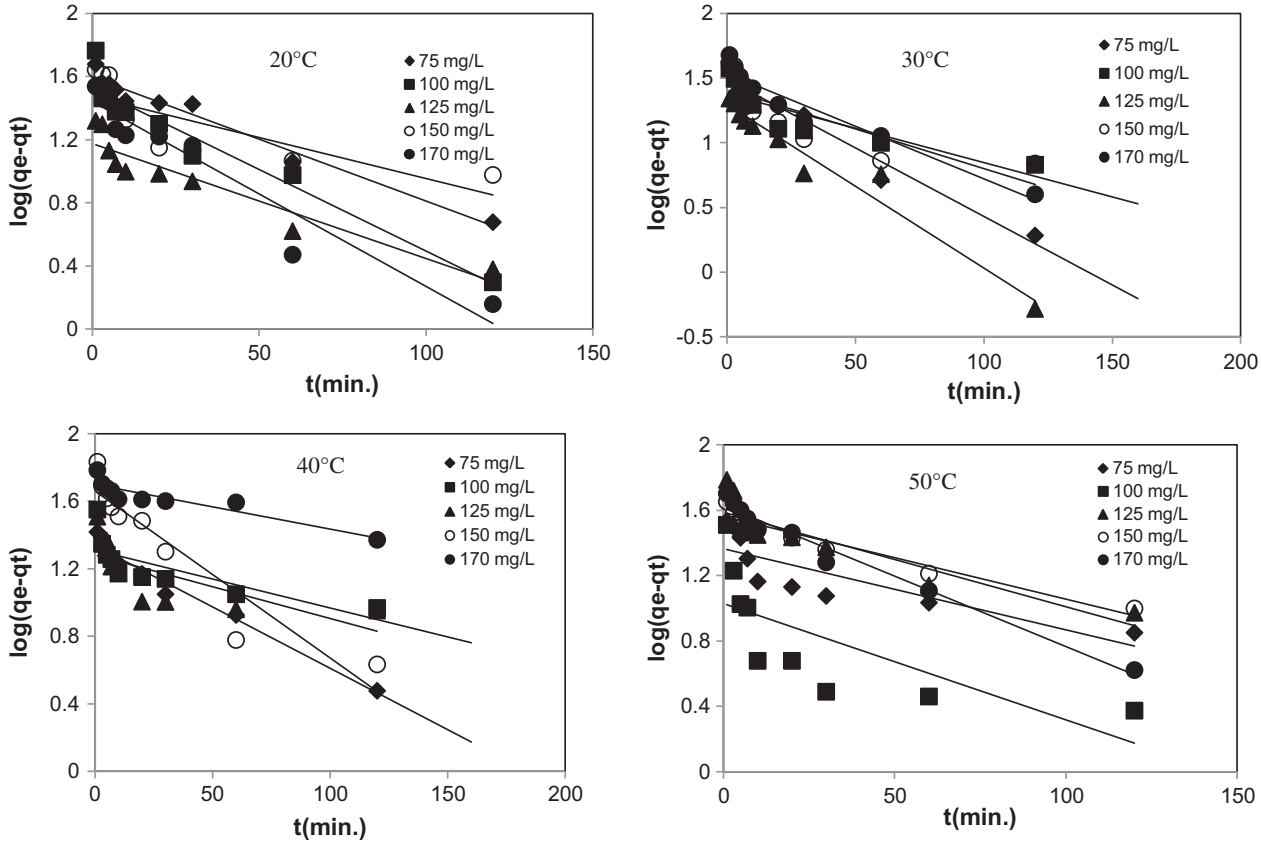

Fig. 13. Pseudo-first-order kinetic models for BV10 adsorption on sawdust of *S. mahagoni* at different initial dye concentrations and temperatures.

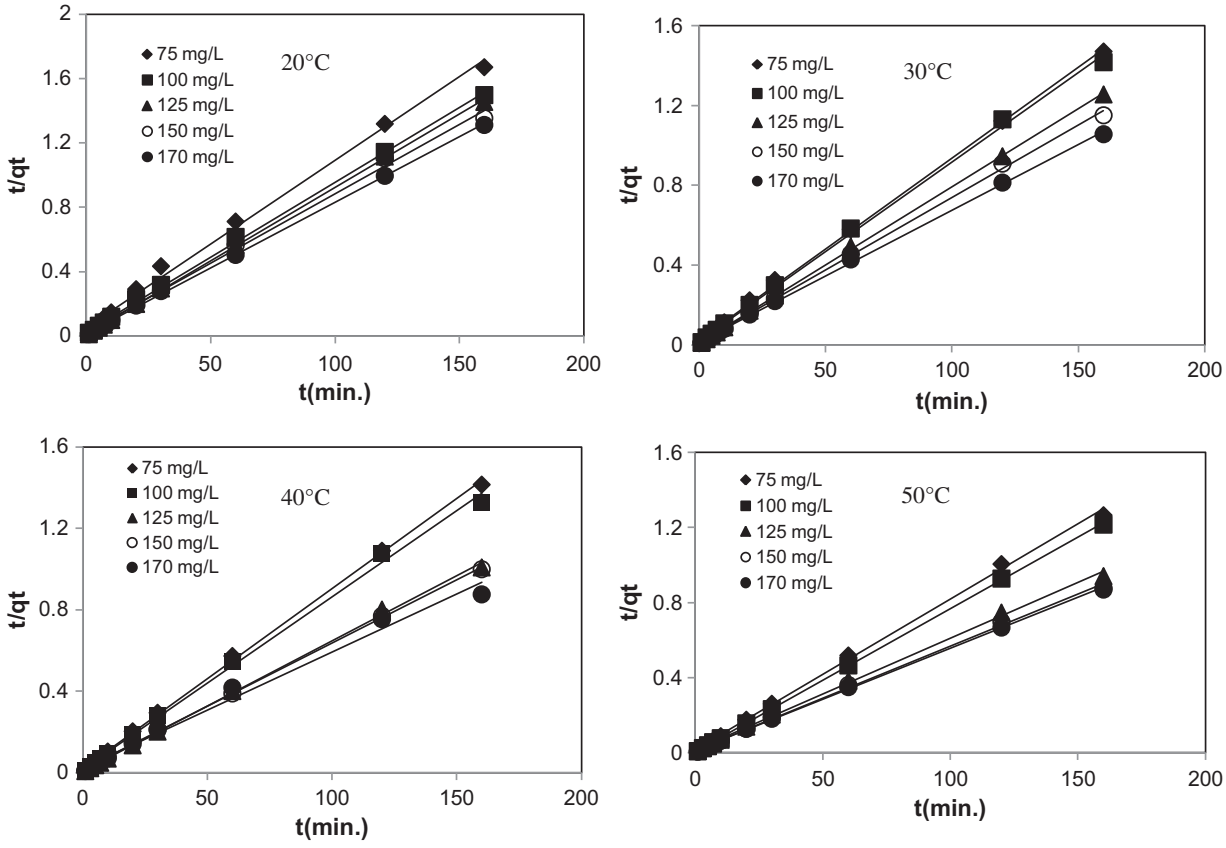

Fig. 14. Pseudo-second-order kinetic models for BV10 adsorption on sawdust of *S. mahagoni* at different initial dye concentrations and temperatures.

significance of Fig. 16 shows the plot q_t vs. ln t having slope $1/b$ and intercept [$(1/b)$ ln (ab)].

As shown in Table 2, the correlation coefficients for BV10 were very low (0.4947–0.97789 and the calculated equilibrium adsorption capacity ($q_{e,cal}$) does not agree with the experimental values ($q_{e,exp}$). This indicates that the adsorption of BV10 onto sawdust of *S. mahagoni* is not an ideal pseudo-first-order reaction.

The $q_{e,exp}$ and the $q_{e,cal}$ values from the pseudo-second-order kinetic model are very close to each other (Table 2). The calculated correlation coefficients (R^2 ~ 0.99) are also close to unity for pseudo-second-order kinetic than those for the pseudo-first-order kinetic model. Therefore, the adsorption can be approximated more appropriately by pseudo-second-order kinetic model than other studied kinetic models. The pseudo-second-order model is based on the assumption that the rate-determining step may be a chemical sorption involving valence forces through sharing or exchange of electrons between adsorbent and sorbate [36].

Values of intercept, C, give an idea about the thickness of boundary layer, i.e. the larger the intercept, the greater is the boundary layer effect [31]. The deviation of the straight lines from the origin, as shown in the figure, may be because of the difference between the rate of mass transfer in the initial and final steps of adsorption. Furthermore, such deviated straight line from the origin indicates that the pore diffusion is not the sole rate-controlling step [1]. From Fig. 15, it may be seen that there are two separate regions; the first portion is attributed to the bulk diffusion and the second portion to intraparticle diffusion.

Based on linear regression (R^2) values, the kinetics of BV10 onto sawdust of *S. mahagoni* can be described well by pseudo-second-order > Elovich > Intraparticle diffusion > pseudo-first-order equation.

3.8. Activation energy and thermodynamic parameters

Represented in Table 2, the pseudo-second-order rate constant k_2, the activation energy E_a for adsorption

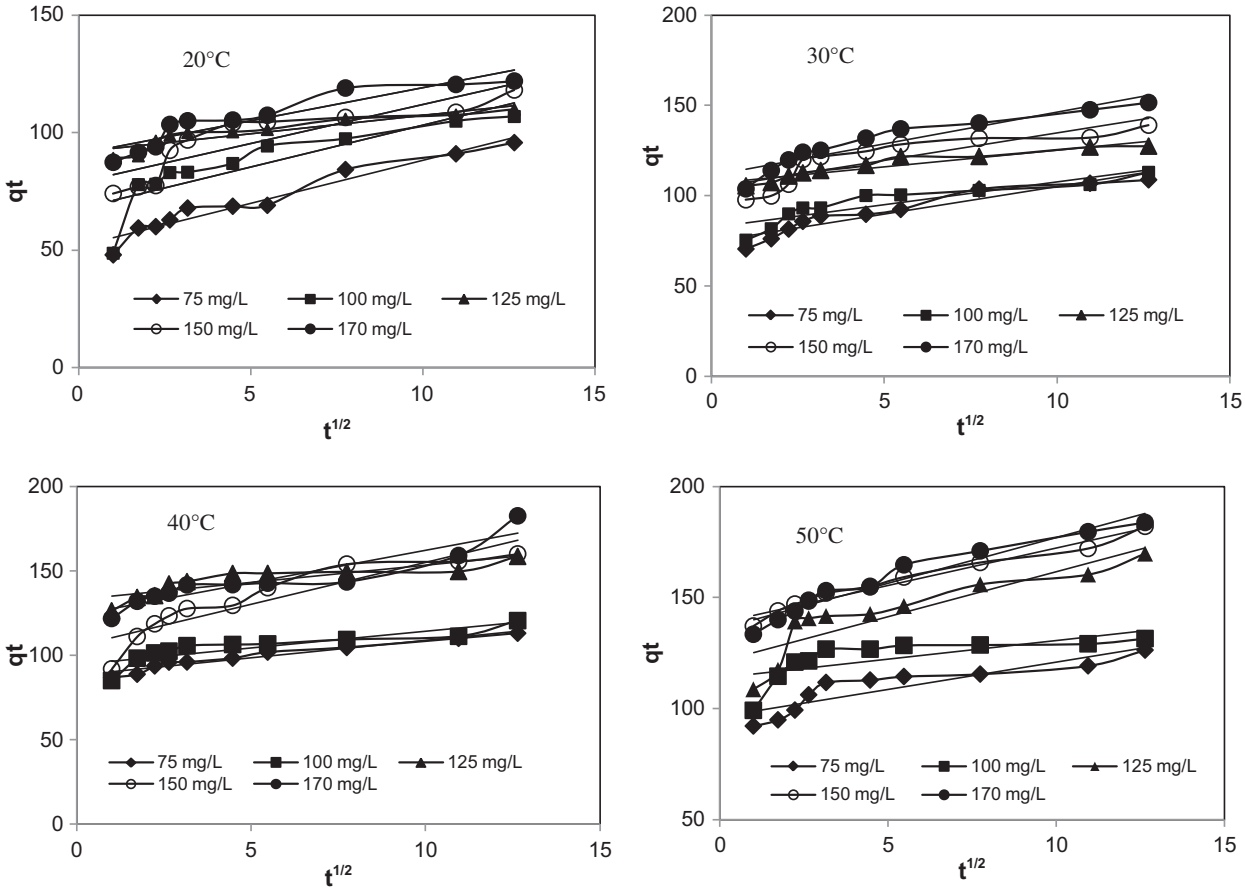

Fig. 15. Intraparticle diffusion kinetic models for BV10 adsorption on sawdust of *S. mahagoni* at different initial dye concentrations and temperatures.

of BV10 onto sawdust of *S. mahagoni* was determined using the Arrhenius equation.

$$\ln k_2 = \ln A - \frac{E_a}{RT} \tag{6}$$

In Eq. (6), E_a is the Arrhenius activation energy (kJ mol^{-1}), A the Arrhenius factor, R the gas constant (8.314 J mol^{-1} K) and T is the solution temperature in Kelvin [26]. By plotting ln k_2 vs. $1/T$, E_a was obtained from the slope of the linear plot and was estimated to be around 20.97 kJ mol^{-1}.

Generally, low-activation energies (5–40 kJ mol^{-1}) are characteristic of physical adsorption, while high ones (40–800 kJ mol^{-1}) suggest chemisorptions [37]. The value of activation energy (52.15 kJ mol^{-1}) shows that the adsorption of BV10 onto sawdust of *S. mahagoni* was a physisorption process.

The thermodynamic parameters of processes such as enthalpy (ΔH°), entropy (ΔS°), and free energy (ΔG°) of dye adsorption on modified sawdust of *S. mahagoni* were calculated by using the following Eqs. (7)–(9) [38]:

$$\mathrm{K_D} = \frac{\text{amount of dye in adsorbent}}{\text{amount of dye in solution}} = \frac{V}{W} \tag{7}$$

$$\Delta G^\circ = -RT \ln K \tag{8}$$

where ΔG° is standard free energy change (J), R the universal gas constant, 8.314 kJ mol^{-1}, and the absolute temperature (K).

$$\Delta G^\circ = \Delta H^\circ - T\Delta S^\circ \tag{9}$$

The plot of ΔG° as a function of T (Fig. 18) a straight line from which ΔH° and ΔS° can be calculated from the slope and intercept, respectively.

As shown in Table 3, the negative values of ΔG° indicate that the adsorption of BV10 on the

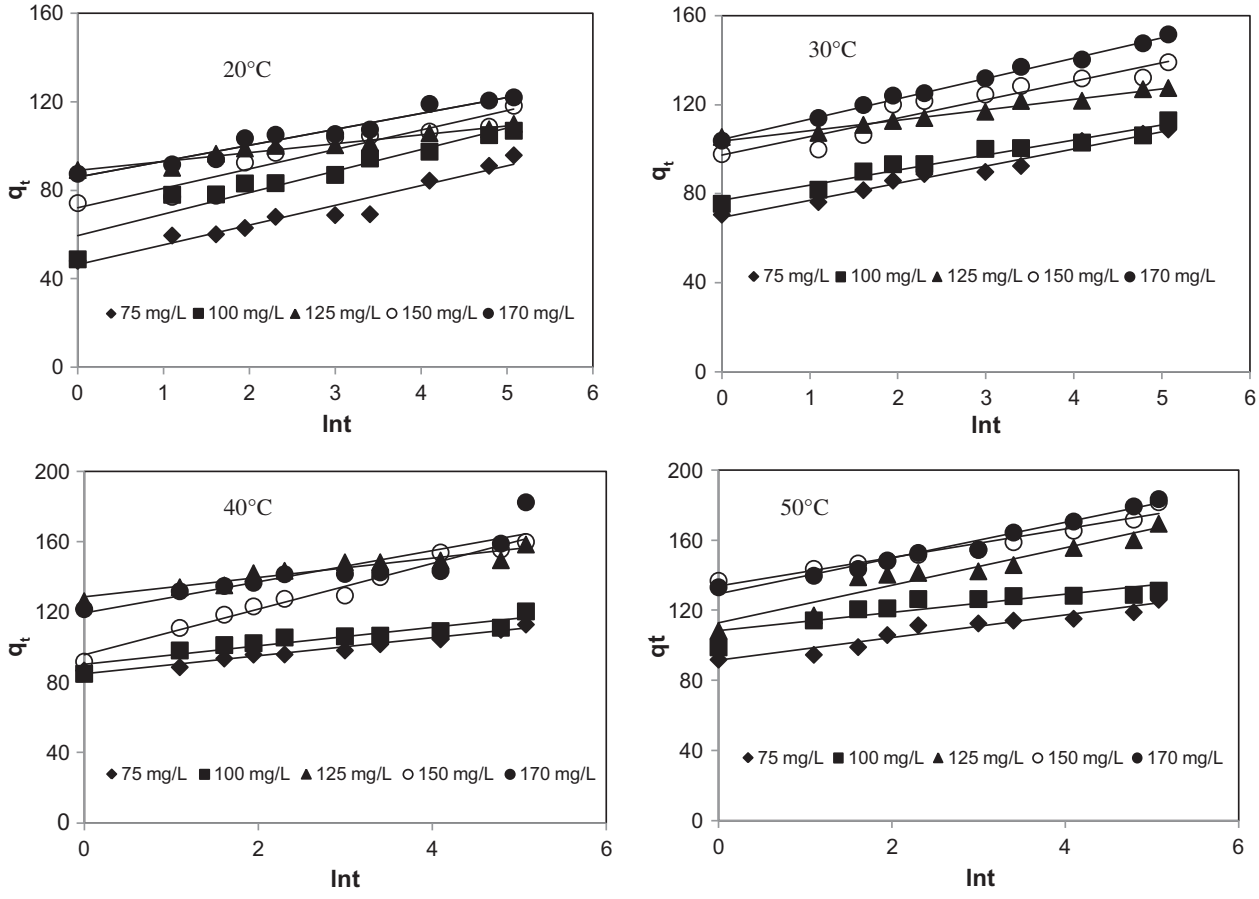

Fig. 16. Elovich equation for BV10 adsorption on sawdust of *S. mahagoni* at different initial dye concentrations and temperatures.

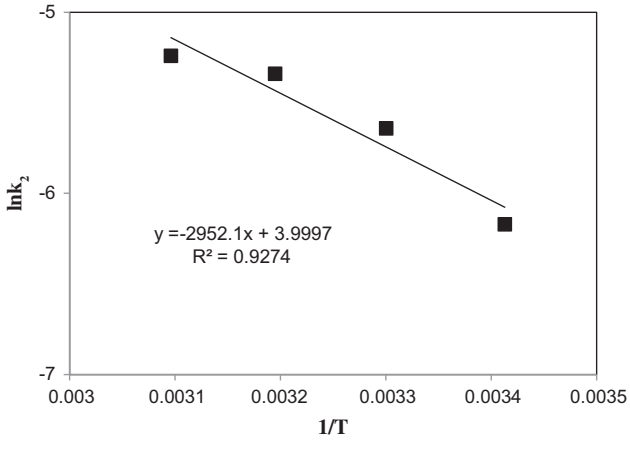

Fig. 17. ln k_2 vs. 1/T for 75 mg L^{-1} BV10 concentration.

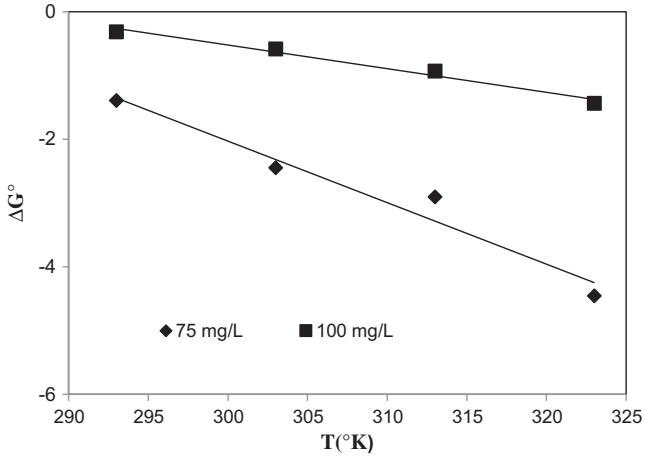

Fig. 18. ΔG° vs. T for the adsorption of BV10 by sawdust of *S. mahagoni*.

sawdust is spontaneous. The magnitude of enthalpy is consistent with a physical interaction of an adsorbent with an adsorbate. The enthalpy changes (ΔH°) indicate that adsorption followed endothermic processes [39]. The positive value of ΔS° indicated an increase in randomness at the solid/solution

Table 3
Thermodynamic parameters of sawdust of *S. mahagoni* at different initial BV10 concentrations

BV10 con. (mgL^{-1})	ΔG°(kJ mol^{-1})				ΔH°(kJ mol^{-1})	ΔS°(kJ mol^{-1})
	293 K	303 K	313 K	323 K		
75	−1.39	−2.45	−2.90	–4.45	26.90	96.4
100	−0.32	−0.58	−0.93	−1.43	10.64	37.1

interface after BV10 adsorption on sawdust of *S. mahagoni* [40].

4. Conclusion

In the present study, sawdust of *S. mahagoni* was used as an effective adsorbent for the removal of BV10 from aqueous solutions. Characterization of adsorbent was carried out which showed the presence of various functional groups on the adsorbent surface and that the adsorbent was mesoporous material and suitable for adsorption. The adsorption equilibrium data fitted well with the Langmuir isotherm model, and kinetic data were fitted by the pseudo-second-order model. The predicted maximum monolayer adsorption capacity of sawdust of *S. mahagoni* from the Langmuir model was 222.76 mg g^{-1} at pH 4.2 and 50°C. Thermodynamic analysis indicated that adsorption of BV10 onto sawdust of *S. mahagoni* was spontaneous and endothermic in nature.

References

[1] R. Ahmad, Studies on adsorption of crystal violet dye from aqueous solution onto coniferous pinus bark powder (CPBP), J. Hazard. Mater. 171 (2009) 767–773.
[2] A. Arunarani, P. Chandran, B.V. Ranganathan, N.S. Vasanthi, S. Sudheer Khan, Bioremoval of Basic Violet 3 and Acid Blue 93 by Pseudomonas putida and its adsorption isotherms and kinetics, Colloid Surface B. 102 (2013) 379–384.
[3] K. Bellir, I.S. Bouziane, Z. Boutamine, M.B. Lehocine, A.H. Meniai, Sorption Study of a Basic Dye "Gentian Violet" from Aqueous Solutions Using Activated Bentonite, Energy Procedia 18 (2012) 924–933.
[4] S. Chen, J. Zhang, C. Zhang, Q. Yue, Y. Li, C. Li, Equilibrium and kinetic studies of methyl orange and methyl violet adsorption on activated carbon derived from Phragmites australis, Desalination 252 (2010) 149–156.
[5] F. Güzel, H. Sayğılı, G.A. Sayğılı, F. Koyuncu, Decolorisation of aqueous crystal violet solution by a new nanoporous carbon: Equilibrium and kinetic approach, J. Ind. Eng. Chem. 20 (2014) 3375–3386.
[6] A. Hassani, L. Alidokht, A.R. Khataee, S. Karaca, Optimization of comparative removal of two structurally different basic dyes using coal as a low-cost and available adsorbent, J. Taiwan I. Chem. Eng. 45 (2014) 1597–1607.
[7] F. Deniz, S.D. Saygideger, Investigation of adsorption characteristics of Basic Red 46 onto gypsum: Equilibrium, kinetic and thermodynamic studies, Desalination 262 (2010) 161–165.
[8] M. El Haddad, R. Mamouni, N. Saffaj, S. Lazar, Removal of a cationic dye—Basic Red 12—from aqueous solution by adsorption onto animal bone meal, J. Assoc. Arab Univ. Basic Appl. Sci. 12 (2012) 48–54.
[9] G.O. El-Sayed, Removal of methylene blue and crystal violet from aqueous solutions by palm kernel fiber, Desalination 272 (2011) 225–232.
[10] E. Eren, B. Afsin, Investigation of a basic dye adsorption from aqueous solution onto raw and pre-treated bentonite surfaces, Dyes Pigments 76 (2008) 220–225.
[11] K.A. Guimarães Gusmão, L.V. Alves Gurgel, T.M. Sacramento Melo, L.F. Gil, Application of succinylated sugarcane bagasse as adsorbent to remove methylene blue and gentian violet from aqueous solutions—Kinetic and equilibrium studies, Dyes Pigments 92 (2012) 967–974.
[12] B.H. Hameed, F.B.M. Daud, Adsorption studies of basic dye on activated carbon derived from agricultural waste: *Hevea brasiliensis* seed coat, Chem. Eng. J. 139 (2008) 48–55.
[13] Y.-X. Jiang, H.-J. Xu, D.-W. Liang, Z.-F. Tong, Adsorption of Basic Violet 14 from aqueous solution on bentonite, Comptes Rendus Chimie 11 (2008) 125–129.
[14] K.C. Tushar, K. Bera, K. Jana, K.M. Ali, S.M. Debasis De, D. Ghosh, Antihyperglycemic and antioxidative effect of hydro-methanolic (2:3) extract of the seed of *Swietenia mahagoni* (L.) Jacq. in streptozotocin-induced diabetic male albinorat: An approach through pancreas, Genomic Medicine 4 (2012) 107–117.
[15] L. Wang, J. Zhang, R. Zhao, C. Li, Y. Li, C. Zhang, Adsorption of basic dyes on activated carbon prepared from Polygonum orientale Linn: Equilibrium, kinetic and thermodynamic studies, Desalination 254 (2010) 68–74.
[16] G. Crini, Kinetic and equilibrium studies on the removal of cationic dyes from aqueous solution by adsorption onto a cyclodextrin polymer, Dyes Pigments 77 (2008) 415–426.
[17] Y. Lin, X. He, G. Han, Q. Tian, W. Hu, Removal of Crystal Violet from aqueous solution using powdered mycelial biomass of Ceriporia lacerata P2, J. Environ. Sci. 23 (2011) 2055–2062.
[18] S. Mona, A. Kaushik, C.P. Kaushik, Waste biomass of Nostoc linckia as adsorbent of crystal violet dye: Optimization based on statistical model, Int. Biodeter. Biodegr. 65 (2011) 513–521.

[19] E. Alver, A.Ü. Metin, Anionic dye removal from aqueous solutions using modified zeolite: Adsorption kinetics and isotherm studies, Chem. Eng. J. 200–202 (2012) 59–67.
[20] F.A. Pavan, E.S. Camacho, E.C. Lima, G.L. Dotto, V.T.A. Branco, S.L.P. Dias, Formosa papaya seed powder (FPSP): Preparation, characterization and application as an alternative adsorbent for the removal of crystal violet from aqueous phase, J. Environ. Chem. Eng. 2 (2014) 230–238.
[21] K.P. Singh, S. Gupta, A.K. Singh, S. Sinha, Optimizing adsorption of crystal violet dye from water by magnetic nanocomposite using response surface modeling approach, J. Hazard. Mater. 186 (2011) 1462–1473.
[22] E. Malkoc, Y. Nuhoglu, Fixed bed studies for the sorption of chromium(VI) onto tea factory waste, Chem. Eng. Sci. 61 (2006) 4363–4372.
[23] J. Fu, Q. He, B. Liu, J. Zhang, B. Hu, Study in adsorption behavior of polymer on molecular sieves by surface and pore properties, Colloids and Surface A. 369 (2010) 113–120.
[24] A. Nilchi, T. Shariati Dehaghan, S. Rasouli Garmarodi, Kinetics, isotherm and thermodynamics for uranium and thorium ions adsorption from aqueous solutions by crystalline tin oxide nanoparticles, Desalination 321 (2013) 67–71.
[25] S. Chen, R. Wang, Surface area, pore size distribution and microstructure of vacuum getter, Vacuum 85 (2011) 909–914.
[26] K. Elass, A. Laachach, A. Alaoui, M. Azzi, Removal of methyl violet from aqueous solution using a stevensite-rich clay from Morocco, App. Clay Sci. 54 (2011) 90–96.
[27] B. Kayranli, Adsorption of textile dyes onto iron based waterworks sludge from aqueous solution; isotherm, kinetic and thermodynamic study, Chem. Eng. J. 173 (2011) 782–791.
[28] A. Saeed, M. Sharif, M. Iqbal, Application potential of grapefruit peel as dye sorbent: Kinetics, equilibrium and mechanism of crystal violet adsorption, J. Hazard. Mater. 179 (2010) 564–572.
[29] N. Thinakaran, P. Baskaralingam, M. Pulikesi, P. Panneerselvam, S. Sivanesan, Removal of Acid Violet 17 from aqueous solutions by adsorption onto activated carbon prepared from sunflower seed hull, J. Hazard Mater. 151 (2008) 316–322.
[30] S. Chakraborty, S. Chowdhury, P. Das Saha, Adsorption of Crystal Violet from aqueous solution onto NaOH-modified rice husk, Carbohydrate Polymers, 86 (2011) 1533–1541.
[31] I.A.W. Tan, A.L. Ahmad, B.H. Hameed, Adsorption of basic dye on high-surface-area activated carbon prepared from coconut husk: Equilibrium, kinetic and thermodynamic studies, J. Hazard. Mater. 154 (2008) 337–346.
[32] X. Wu, K.N. Hui, K.S. Hui, S.K. Lee, W. Zhou, R. Chen, D.H. Hwang, Y.R. Cho, Y.G. Son, Adsorption of basic yellow 87 from aqueous solution onto two different mesoporous adsorbents, Chem. Eng. J. 180 (2012) 91–98.
[33] L. Zhou, J. Huang, B. He, F. Zhang, H. Li, Peach gum for efficient removal of methylene blue and methyl violet dyes from aqueous solution, Carbohydrate Polymers 101 (2014) 574–581.
[34] P. Wang, M. Cao, C. Wang, Y. Ao, J. Hou, J. Qian, Kinetics and thermodynamics of adsorption of methylene blue by a magnetic graphene-carbon nanotube composite, Appl. Surface Sci. 290 (2014) 116–124.
[35] Sumanjit S. Rani, R.K. Mahajan, Equilibrium, kinetics and thermodynamic parameters for adsorptive removal of dye Basic Blue 9 by ground nut shells and Eichhornia, Arabian J. Chem. (in press).
[36] G. Bayramoglu, B. Altintas, M.Y. Arica, Adsorption kinetics and thermodynamic parameters of cationic dyes from aqueous solutions by using a new strong cation-exchange resin, Chem. Eng. J. 152 (2009) 339–346.
[37] H. Tang, W. Zhou, L. Zhang, Adsorption isotherms and kinetics studies of malachite green on chitin hydrogels, J. Hazard. Mater 209–210 (2012) 218–225.
[38] R. Aravindhan, J.R. Rao, B.U. Nair, Removal of basic yellow dye from aqueous solution by sorption on green alga Caulerpa scalpelliformis, J. Hazard. Mater. 142 (2007) 68–76.
[39] T. Calvete, E.C. Lima, N.F. Cardoso, S.L.P. Dias, F.A. Pavan, Application of carbon adsorbents prepared from the Brazilian pine-fruit-shell for the removal of Procion Red MX 3B from aqueous solution—Kinetic, equilibrium, and thermodynamic studies, Chem. Eng. J. 155 (2009) 627–636.
[40] M.A.K.M. Hanafiah, W.S.W. Ngah, S.H. Zolkafly, L.C. Teong, Z.A.A. Majid, Acid Blue 25 adsorption on base treated Shorea dasyphylla sawdust: Kinetic, isotherm, thermodynamic and spectroscopic analysis, J. Environ. Sci. 24 (2012) 261–268.